Biochimica et Biophysica Acta 1828 (2013) 1962–1972

Contents lists available at SciVerse ScienceDirect

Biochimica et Biophysica Acta

journal homepage: www.elsevier.com/locate/bbamem

Lipid and phase specificity of α-toxin from *S. aureus*

M. Schwiering, A. Brack, R. Stork, N. Hellmann *

Institute for Molecular Biophysics, Jakob-Welder-Weg 26, University of Mainz, 55128 Mainz, Germany

ARTICLE INFO

Article history:
Received 19 October 2012
Received in revised form 5 April 2013
Accepted 8 April 2013
Available online 13 April 2013

Keywords:
Pore formation
Oligomerisation
Toxin
S. aureus
Artificial membranes

ABSTRACT

The pore forming toxin Hla (α-toxin) from *Staphylococcus aureus* is an important pathogenic factor of the bacterium *S. aureus* and also a model system for the process of membrane-induced protein oligomerisation and pore formation. It has been shown that binding to lipid membranes at neutral or basic pH requires the presence of a phosphocholine-headgroup. Thus, sphingomyelin and phosphatidylcholine may serve as interaction partners in cellular membranes. Based on earlier studies it has been suggested that rafts of sphingomyelin are particularly efficient in toxin binding. In this study we compared the oligomerisation of Hla on liposomes of various lipid compositions in order to identify the preferred interaction partners and conditions. Hla seems to have an intrinsic preference for sphingomyelin compared to phosphatidylcholine due to a higher probability of oligomerisation of membrane bound monomer. We also can show that increasing the surface density of Hla-binding sites enhances the oligomerisation efficiency. Thus, preferential binding to lipid rafts can be expected in the cellular context. On the other hand, sphingomyelin in the liquid disordered phase is a more favourable binding partner for Hla than sphingomyelin in the liquid ordered phase, which makes the membrane outside of lipid rafts the more preferred region of interaction. Thus, the partitioning of Hla is expected to strongly depend on the exact composition of raft and non-raft domains in the membrane.

1. Introduction

Pore forming toxins play an important role in the attack of target cells by bacteria and animals. Typically these molecules (peptides or proteins) are secreted into the surrounding medium as monomers. Binding of these pathogenic factors disturbs membrane integrity by formation of a transmembrane pore, in many cases via the assembly of several toxin molecules to an oligomeric complex. These pores vary strongly in size, depending on the type of toxin and number of protomers in the final oligomeric structure [1,2]. The initial contact with the cell membrane is made via certain protein receptors and/or lipid components, depending on the toxin type and concentration (see Ref. [2] for an overview). In case of toxin binding to lipid headgroups a frequently identified receptor structure is the phosphocholine (POC) headgroup which is abundant on the outer leaflet of the plasma membrane in form of unsaturated phosphatidylcholine (PC) and saturated sphingomyelin (SM). In a couple of cases binding of toxin occurs preferentially to SM and is further increased by availability of cholesterol [3–5].

The toxin Hla from *Staphylococcus aureus* also requires POC-carrying lipids for interaction with liposomes [6]. This toxin belongs to the class of β-barrel forming toxins, which share a strong structural similarity with β-barrel membrane proteins such as outer-membrane proteins or porins [7]. The high resolution structure of the heptameric pore of Hla, obtained in presence of detergents, reveals a putative binding site for a phosphocholine-headgroup [8,9]. One can assume that this binding site also plays a role for the interaction of Hla monomers with membranes, but detailed information about this process is lacking. Also, the intermediate oligomeric states have not been characterised yet. Despite numerous studies the large range of susceptibilities of cells even of the same type [10] is not understood. Different proteins have been suggested to be involved in Hla binding: band-3 [11], caveolin-1 [12] and ADAM10 [13]. However, high affinity binding of Hla directly to these proteins could not be proven so far. Based on the role of SM and cholesterol for the interaction of Hla with highly susceptible rabbit erythrocytes and with artificial membranes, an alternative type of high affinity binding site was proposed: clustering of low affinity binding sites (POC) due to formation of domains enriched in sphingomyelin and cholesterol was suggested to effectively increase the surface density of monomeric Hla and thus reduce the concentration of toxin required to yield oligomers and pores [14].

The aim of our study was to investigate to which extent domains enriched in sphingomyelin and cholesterol increase Hla binding and

Abbreviations: LUV, large unilamellar vesicle; GUV, giant unilamellar vesicle; POC, phosphocholine; SM, sphingomyelin; eSM, egg yolk N-acyl-D-sphingosine-1-phosphocholine; OSM, N-(9Z-octadecenoyl)-sphing-4-enine-1-phosphocholine; bPS, 1,2-diacyl-*sn*-glycero-3-phospho-L-serine from bovine brain; ePE, egg yolk 1,2-diacyl-*sn*-glycero-3-phosphoethanolamine; PC, phosphatidylcholine; ePC, egg yolk 1,2-diacyl-*sn*-glycero-3-phosphocholine; Chol, cholesterol; DPPC, 1,2-dipalmitoyl-*sn*-glycero-3-phosphocholine; DSPC, 1,2-Distearoyl-*sn*-Glycero-3-Phosphocholine; PM, pyrene-maleimide; [eSM_{ol}], [ePC_{ol}], concentration of eSM/ePC in the outer leaflet of the liposome; SDS, sodium dodecyl sulphate

* Corresponding author at: Institute for Molecular Biophysics, Jakob-Welder-Weg 26, 55128 Mainz, Germany. Tel.: +49 6131 392 3567; fax: +49 6131 392 3557.
E-mail address: nhellmann@uni-mainz.de (N. Hellmann).

0005-2736/$ – see front matter © 2013 Elsevier B.V. All rights reserved.
http://dx.doi.org/10.1016/j.bbamem.2013.04.005

oligomerisation and which properties are the reasons for the enhancement. To this end the interaction of Hla with liposomes of different compositions was monitored based on pyrene-excimer fluorescence of Hla. To address the influence of local density of binding sites the liposomes contained Hla-binding lipids were mixed with non-binding lipids in different relative amounts. In order to test for lipid specificity of Hla-binding, the interaction with sphingomyelin and phosphatidylcholine was compared. The influence of lipid phase was investigated by using both saturated and unsaturated species of sphingomyelin and phosphatidylcholine. To qualitatively interpret the results an approximate model describing binding of monomers and formation of dimers on the membrane was developed. The results show clearly that the surface density of binding sites modulates the efficiency of oligomerisation but that the extent of Hla binding primarily depends on lipid identity (sphingomyelin or phosphatidylcholine) and lipid phase.

2. Materials and methods

2.1. Chemicals

Egg yolk 1,2-diacyl-*sn*-glycero-3-phosphocholine (ePC), egg yolk 1,2-diacyl-*sn*-glycero-3-phosphoethanolamine (ePE), egg yolk N-acyl-D-sphingosine-1-phosphocholine (eSM), 1,2 diacyl-*sn*-glycero-3-phospho-L-serine from bovine brain (bPS), 1,2-dipalmitoyl-*sn*-glycero-3-phosphocholine (DPPC) and cholesterol were obtained from Sigma (Deisenhofen, Germany). N-(9Z-octadecenoyl)-sphing-4-enine-1-phosphocholine (OSM), 1,2-Distearoyl-*sn*-Glycero-3-Phosphocholine (DSPC) and 1,2-dioleoyl-*sn*-glycero-3-phosphoethanolamine-N-(lissamine rhodamine B sulfonyl) (Lissamine rhodamine DOPE) were purchased from Avanti Polar Lipids (Alabaster, Alabama, USA). Chemicals for the buffer solution and SDS PAGE were from Roth GmbH (Karlsruhe, Germany). All experiments were performed in phosphate buffer (70 mM sodium phosphate, pH 7.2).

2.2. Toxin labelling

For fluorescence dye labelling the Hla mutant S3C was used, where serine on the third position of the amino acid sequence is replaced by cysteine. This fully active mutant S3C was produced and labelled with N-3′-pyrenyl-maleimide (PM, Molecular Probes, Eugene, OR) as described elsewhere [15]. Toxin was kept at −80 °C, slowly thawed on ice and used directly. Concentration of the eluted protein was determined based on a variable extinction coefficient taking into account incomplete labelling ($c = (A_{280} - 0.73A_{340})/\varepsilon l$ with ε the molar extinction coefficient for unlabelled toxin ($\varepsilon = 65\,000\ M^{-1}\ cm^{-1}$ as determined from the amino acid sequence) and l the optical pathlength). The absorbance spectrum of pyrene-maleimide conjugated with protein was determined from a spectrum of the PM-mercaptoethanol-adduct. From this we calculated that pyrene-maleimide conjugated with protein exhibits at 280 nm an absorbance which is 0.73× the value observed at 340 nm.

2.3. Vesicle preparation

Extruded vesicles (100 nm filter, extruder from Avanti Polar Lipids, Alabaster, Alabama, USA) with different relative amounts (expressed as mol %) of ePE, bPS, PC, SM and cholesterol were prepared in phosphate buffer essentially as described elsewhere [14]. Mixtures containing cholesterol plus one type of lipid are denoted binary mixtures, those containing bPS, ePE, cholesterol and ePC or OSM are referred to as pseudo-binary mixtures, and those containing bPS, ePE, cholesterol and DPPC, DSPC or eSM pseudo-ternary. These LUVs were used for all experiments except for fluorescence microscopy. Size and monodispersity of the LUV suspension was routinely checked with dynamic light scattering (Zetasizer Nano ZS, Malvern Instruments GmbH, Herrenberg, Germany) and found to vary only slightly with preparation. The actual lipid concentration was determined via the cholesterol content employing the CHOD PAP assay (Roche diagnostics GmbH, Mannheim, Germany). Based on the amount of cholesterol in the suspension the concentration of lipids was calculated. Thin layer chromatography had proven that the actual lipid composition of this type of liposomes agrees with the intended one [16], allowing calculation of the lipid concentration based on this strategy. For efflux measurements liposomes were prepared in 70 mM phosphate-buffer, pH 7.2 containing additionally the self-quenching dye carboxyfluorescein (Fluka, Sigma Aldrich, Germany) in a concentration of 50 mM. The dye outside the liposomes was removed employing desalting columns (PD10, Amersham Biosciences Europe GmbH, Freiburg, Germany).

2.4. Fluorescence measurements

Spectra were obtained in micro-quartz cuvettes (volume 400 µl, Hellma GmbH & Co, Müllheim, Germany) at an excitation wavelength of 335 nm and emission wavelengths between 350 and 600 nm at the temperature indicated. Fluorescence spectra were measured with a Hitachi F4500 (Binninger Analytic, Schwaebisch Gmuend, Germany) or a Fluorolog II (Horiba Scientific, Unterhaching, Germany). Spectra of liposomes without toxin were subtracted before data evaluation. The liposomes were incubated at the Hla and lipid concentration as indicated, but diluted to 0.1 µM directly before the measurement if incubation concentrations of Hla were higher than 0.1 µM. In a few cases the samples were measured without dilution (Fig. 3b) and the results were basically the same, indicating that no significant dissociation occurs. Furthermore, the sum of dissociation rate of monomers and oligomers was estimated to be $<0.01\ s^{-1}$, corresponding to a half-life of the oligomers of >100 s (see Results). Thus, the fluorescence signal as measured under these conditions represents the situation characteristic for the incubation concentrations. Fluorescence data were always measured at 20 °C, irrespective of incubation temperature in order to allow comparison of fluorescence intensity. Concentration of Hla-binding lipids (PC and SM) is given in terms of the fraction available for Hla-binding, e.g. only those on the outer leaflet of the liposomes.

In cases, where the results of several experiments were plotted together, the amount of excimers formed was quantified by calculation of the excimer peak area (430 to 600 nm) relative to the total area, indicated as F_{rel}^{olig}. Otherwise, the fluorescence of the excimer peak was plotted directly, indicated by F_{475}.

The amount of SDS-stable oligomers was compared between different experimental conditions by measuring the excimer fluorescence after addition of 100 µl of a 10% SDS solution to 400 µl solution containing Hla and liposomes. Fluorescence of monomeric Hla in absence of lipids typically increases by a factor 1.4–1.5 upon addition of SDS. However, the excimer fluorescence is much less affected by presence of detergents than monomer fluorescence [17]. Thus, the relative residual excimer fluorescence is expected to be reduced even if none of the oligomers dissociate due to the detergent, but the exact ratio is not known. However, the signal serves only for comparison among the different lipid mixtures. Alternatively, SDS stable oligomers were detected employing SDS–PAGE [18], but omitting heating of the sample. Gels were stained according to [19].

2.5. Stopped flow experiments

Fast reactions were followed with a SF 61DX2 (TgK Scientific Limited, Bradford upon Avon, UK) stopped-flow apparatus with a high band-filter (cut-off 455 nm) in the fluorescence channel at an excitation wavelength of 335 nm. Toxin and Hla-binding lipid concentrations refer to the concentration in the cell after mixing. Concentrations of Hla-binding lipid reflect only the fraction of the lipids present in the outer leaflet.

2.6. Fluorescence microscopy

GUVs were produced in water following an electroformation protocol on ITO slides (Sigma Aldrich, Germany) with details as described earlier [16]. Phase separation was monitored employing the fluorescently labelled lipid Lissamine rhodamine-DOPE (0.1 mol %, Avant Polar Lipids, Alabaster, Alabama, USA) which preferentially partitions into the liquid disordered phase. Fluorescence micrographs were taken with a Keyence BZ-8000 fluorescence microscope (Keyence, Neu-Isenburg, Germany; Filtersets: $\lambda_{ex} = 560/40$; $\lambda_{em} = 630/60$).

3. Results

Oligomerisation of Hla on liposomes (LUVs) of different compositions was followed employing the formation of excimer fluorescence of pyrene-labelled Hla. The aim was to dissect the contributions of type of Hla binding lipid, its surface density and its phase with respect to efficiency of Hla binding and oligomerisation.

3.1. Binding of monomers is fast and weak

The kinetics of excimer-formation determined in stopped-flow experiments could be well fitted with 1, 2 or 3 exponential functions, depending on the time range and the extent of oligomerisation (Fig. 1). This indicates that no lag-phase occurs since this requires different types of functions to describe the data. Thus, oligomerisation starts immediately after mixing, implying that monomer binding occurs within the dead-time of the instrument (about 3 ms). If monomer binding was slow compared to oligomer formation, a lag-phase in the excimer-signal would result since this represents the time required to accumulate enough membrane bound monomers for measurable amounts of oligomers. Since such a lag-phase was not detected in any of the stopped-flow experiments (Figs. 1, 4, and 7), at the toxin concentration employed in these experiments ($\geq$0.3 μM) the process of monomer binding is close to equilibrium prior to oligomerisation. For liposomes containing 40% cholesterol, 40% eSM, 10% ePE and 10% bPS kinetics was followed at different eSM and toxin concentrations (Fig. 1a,b). The largest rate constant, denoted by k_{obs}, reflects the initial phase and increases with lipid and toxin concentration (Fig. 1c). While an increase with toxin concentration is certainly expected the reason for the observed dependence on lipid-concentration is less clear. Thus, in order to qualitatively describe the oligomerisation behaviour of Hla on a membrane, we developed a model for monomer

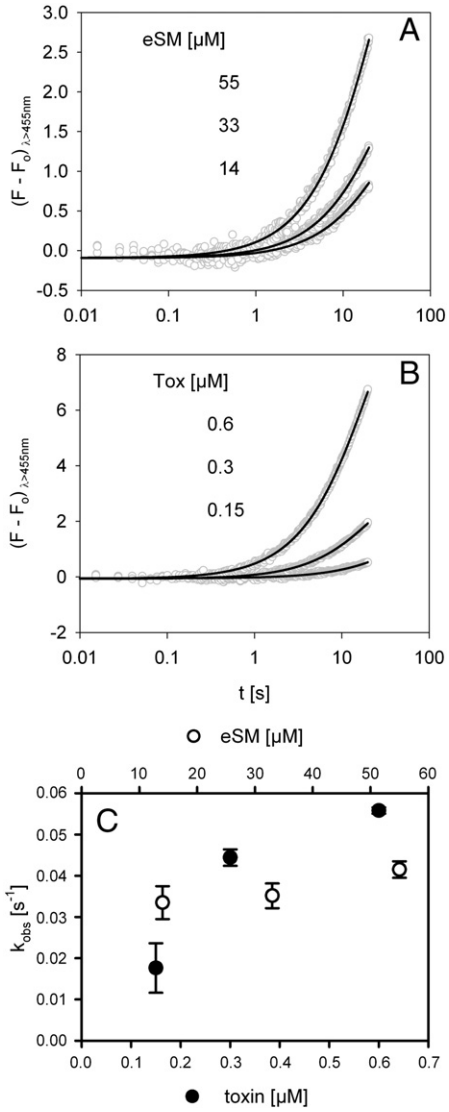

Fig. 1. Kinetics of excimer formation for different concentrations of Hla and eSM. Liposomes containing 40% eSM, 40% cholesterol, 10% ePE and 10% bPS were rapidly mixed with fluorescently labelled toxin at 20 °C. Excimer fluorescence after subtraction of the initial value (F_o) is depicted. The grey symbols represent the data, the black lines a fit based on a mono exponential function ($F = a + b(1 - \exp(-k_{obs}{}^{*}t))$). Panel A depicts data obtained at fixed toxin concentration (0.3 μM) and variable concentration of eSM (number given refer to the concentration of eSM in the outer membrane [eSM_{ol}]). Panel B depicts data obtained at fixed concentration of eSM ([eSM_{ol}] = 17 μM) and variable toxin concentration. In panel C the kinetic constants (k_{obs}) are summarized. Error bars are as estimated by the fitting procedure.

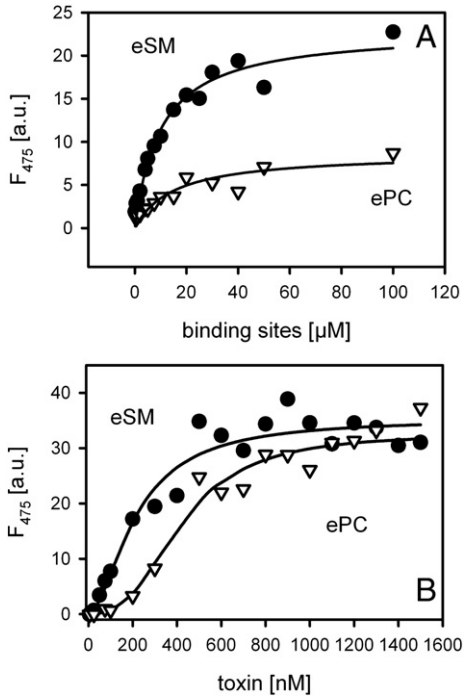

Fig. 2. Concentration dependence of oligomer formation. Liposomes containing 40% cholesterol, 10% bPS, 10% ePE and either 40% ePC (open triangles) or 40% eSM (closed circles) were incubated with pyrene labelled toxin for 24 h at 4 °C. Panel A: Data obtained at constant toxin concentration (4 μM) and variable concentration of binding sites (concentration of eSM or ePC on the outer leaflet, respectively). The black curves represent a fit based on a hyperbolic function (see Eq. (A7)) with $c_{50} = 10 \pm 2$ μM, $F_o = 23 \pm 1$ (eSM) and $c_{50} = 15 \pm 5$ μM, $F_o = 9 \pm 1$ (ePC). Panel B depicts data obtained at constant concentration of Hla-binding lipids: [eSM_{OL}] = [ePC_{OL}] = 2.5 μM. The lines represent a fit based on the Hill-equation (Eq. (A8)) with $c_{50} = 210 \pm 30$ nM (eSM) and $c_{50} = 480 \pm 60$ nM (ePC). The fit is only used to estimate c_{50} (see text for details).

binding to membranes followed by dimerisation. Only in this case analytical solutions for the time-dependent and equilibrium concentration of dimers can be obtained. Whenever this model is used for discussing the results, we refer to "dimer" and "dimerisation constant", in order to distinguish the model from the experimental data, which certainly include also higher oligomers.

Comparison of the trends in k_{obs} as experimentally observed with the equation describing k_{obs} in a dimer-model (Eq. (A6)), reveals that the results of the kinetic experiments are in accordance with a situation where oligomerisation occurs from a pool of bound monomers which are in rapid equilibrium with free monomers (see Appendix A, Eq. (A6)). The dependence on eSM-concentration is weaker than the dependence on the toxin concentration, as can also be rationalised by inspecting Eq. (A6). Based on these experiments we can estimate that the sum of dissociation-rate for oligomers and monomers is smaller than about 0.01 s^{-1}, corresponding to a half-life of about > 100 s.

In order to obtain information about the level of oligomers under equilibrium conditions, pyrene excimer formation was also determined after prolonged incubation (24 h, 4 °C) for different toxin and Hla-binding lipid concentrations (Fig. 2). Here, a low temperature (4 °C) was chosen for two reasons: first, due to the slow rate of oligomer formation at low toxin concentrations, long incubation times were needed to obtain a measurable amount of excimer fluorescence. Unfortunately, at elevated temperatures the toxin is not stable at extended incubation times. However, the oligomerisation process itself is only weakly temperature dependent (see below); thus the results obtained at low temperature are representative for the general oligomerisation behaviour. Secondly, at low temperatures the transition to the lytic pore is strongly suppressed; thus the excimer signal stems mainly from non-pore oligomers on which we would like to focus here (see also Fig. 7).

The curve obtained at low toxin concentration (100 nM) and different Hla-binding lipid concentrations (Fig. 2a) showed that about 10–15 μM Hla-binding lipid is required to achieve half-maximal oligomer formation. The curves can be well described by a hyperbolic curve (Eq. (A7)) with a c_{50} value of 10 ± 2 μM for eSM and c_{50} = 15 ± 5 μM for ePC. However, since excimer fluorescence requires formation of at least a dimer the c_{50} does not correspond to the monomer binding constant K_b, but reflects a combination of K_b and the equilibrium constants describing the oligomerisation process. The

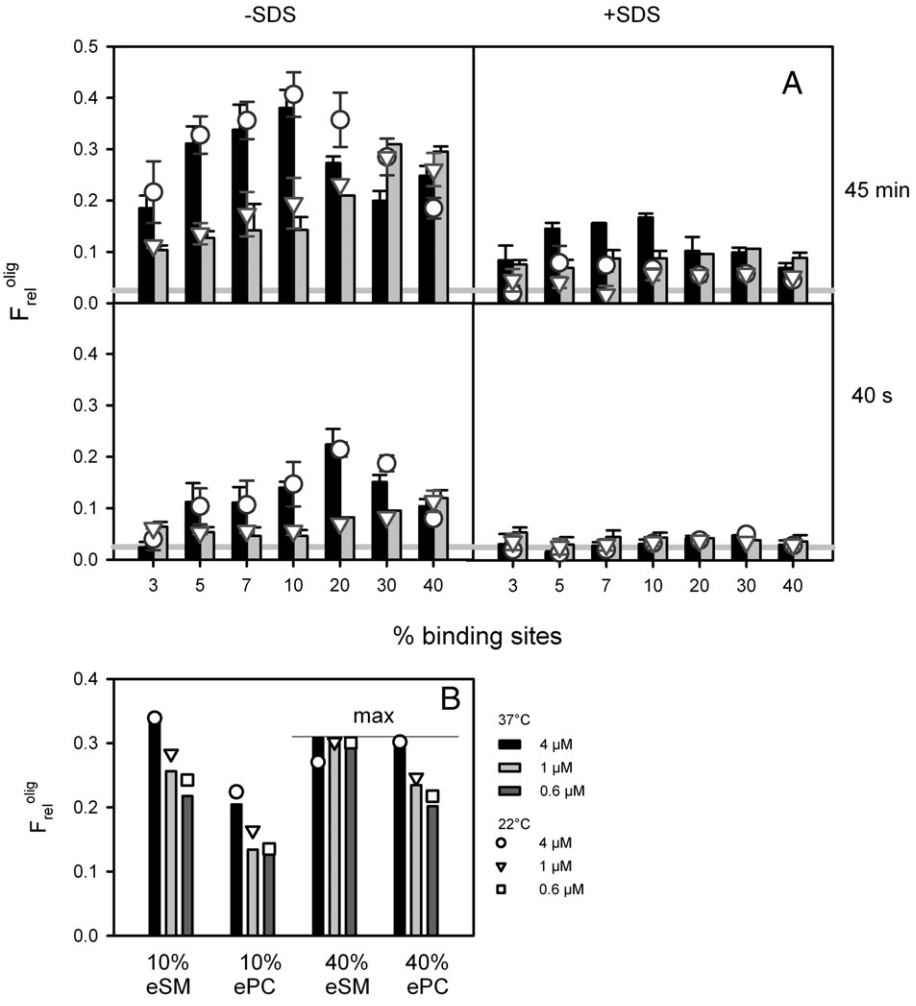

Fig. 3. Enhancement of oligomerisation by surface density. Liposomes containing different fractions of Hla-binding lipid (eSM or ePC) were incubated with pyrene labelled Hla for 40 s or 45 min, at 22 °C or 37 °C. For estimation of the SDS stable oligomers, which includes the pores, excimer fluorescence (at 475 nm) was measured in presence of 2% SDS. Concentration of Hla binding lipids was kept constant at 17 μM (corresponding to the lipid molecules in the outer leaflet) by appropriate dilution of the liposomes. Panel A: Excimer fluorescence obtained at 37 °C is depicted by bars (black: eSM; grey: ePC), results obtained at 22 °C are depicted as symbols (circles: eSM; triangles: ePC).The grey line indicates the level of pyrene fluorescence measured in absence of liposomes. Samples were incubated at 4 μM Hla and diluted to 0.1 μM directly before the measurement. Panel B: Excimer fluorescence was measured after 45 min incubation time at 22 °C (symbols) or 37 °C (bars) for different concentrations of Hla. Note that for liposomes containing 40% eSM or ePC the maximal loading capacity seems to be reached. In case of ePC this level requires a higher toxin concentration than in case of eSM. Samples were incubated at the toxin concentration given, and also measured at this concentration.

hyperbolic shape is not what one would expect, since at sufficiently high lipid concentrations bound monomers should be sufficiently diluted on the liposome surface to reduce visibly the formation of dimers. Based on simulations we can show that the occurrence of a hyperbolic curve in this lipid-concentration range is a clear indication for a low monomer binding affinity. Our simulation was again based on the simplified model of dimer formation, and demonstrates for which combinations of K_d and K_{dim} such a hyperbolic binding curve can be expected (Fig. A1a,b). A hyperbolic shape is observed at a value for K_b of 0.01 μM^{-1} for a range of dimerisation constants (100–5000 nm^2, Fig. A1a). In contrast, already at $K_b = 0.1\ \mu M^{-1}$ a decrease in dimers at higher lipid concentration is predicted (Fig. 1Ab). Thus, we can deduce that for both lipids (eSM and ePC) monomer binding is rather weak. Compared to eSM the K_{50} for ePC is slightly shifted and the maximal level of oligomeric species is visibly decreased. In frame of a dimer model, this combination indicates that the dimerisation constant is lower in case of ePC but the K_b is similar (see Appendix A, Fig. A1c and d).

Variation of toxin concentration at fixed concentration of binding sites (2.5 μM eSM and ePC, respectively, Fig. 2b) supports the findings above: in case of ePC a clear sigmoid shape of the saturation curve is observed, whereas in case of eSM the curve seems to be nearly hyperbolic since the sigmoid part is shifted towards lower concentrations of toxin. The concentration of total toxin needed to achieve half saturation is about 210 nM for eSM and 480 nM for ePC as determined by fitting a Hill-equation (Eq. (A8)) to the data. These values reflect the concentration of toxin necessary to obtain half maximal occupation of the liposomes. Based on purely geometric considerations (see Appendix A) the surface of the liposomes could carry maximally about 240 nM toxin at the lipid concentration employed. Thus, if at 210 nM total toxin concentration 50% of these "binding sites" are occupied, the apparent K_d value is 210 − 120 = 90 nM. In case of ePC a value of 480 − 120 = 360 nM is obtained. These K_d values reflect the average of dissociation constants of the different oligomerisation states present at 50% occupation. The comparison of the results based on Fig. 2a and b clearly demonstrates that the average affinity for binding is increased by at least a factor of 100 upon formation of oligomers.

3.2. Modulation of oligomerisation by surface density of binding sites

The oligomerisation level should increase if the same number of bound monomers is distributed over a smaller number of liposomes. Thus we compared the interaction of Hla with liposomes under conditions where all parameters are constant except the average distance of bound monomers on the liposome surface. This was achieved by changing the fraction of Hla receptor lipids (corresponding to the parameter α in Eq. (A4)). Thus, either ePC or eSM was mixed with lipids which do not bind to Hla (ePE, bPS) and cholesterol (40%) at various fractions. In each case the concentration of binding sites for the toxin (ePC or eSM) was kept constant.

If ePC, which is in the liquid disordered phase at the experimental temperature, was mixed with ePE, bPS and cholesterol, a significant oligomer formation was only obtained at a high fraction of ePC (Fig. 3a), indicating that a certain surface density is required for effective monomer-monomer interaction. If ePC is substituted by eSM, which has a phase transition temperature ($T_{trans} = 41$ °C) well above the experimental temperature (22 °C and 37 °C), a higher concentration of oligomers was found at the same average surface density of Hla-binding lipid except at the highest fraction of ePC and eSM, respectively, where the level is similar. For example in order to achieve the level of oligomer formation obtained with liposomes containing 3% eSM after 45 min, a 7-times higher fraction (20%) is required in case of ePC. The drop of excimer fluorescence at higher eSM fractions in comparison to 10% eSM can be attributed to limitations of the total liposome surface at the concentration employed in this study, since a higher fraction of Hla-binding lipids implies a lower number of liposomes in order to keep the concentration of lipids constant. If a lower concentration of toxin is employed (<1 μM) the excimer fluorescence intensity at 10% eSM is typically lower than at 40% eSM (Fig. 3b). In agreement with the experimental results geometric considerations (see Appendix A) also indicate, that only about 1.6 μM toxin can be accommodated by the liposomes containing 40% ePC or eSM at the given lipid concentration. The differences observed between ePC and eSM were similar for two temperatures (22 °C and 37 °C), two incubation times (about 40 s and 45 min) and also for two types of species: all oligomeric forms (before addition of SDS) and SDS stable oligomers (after addition of SDS). After addition of SDS, only SDS-stable oligomers, which include the pores, exhibit pyrene-excimer fluorescence, and thus as expected the level of excimer fluorescence is higher at an incubation temperature of 37 °C compared to 22 °C, unlike the pyrene-excimer fluorescence before addition of SDS, which is very similar at both temperatures.

The kinetics of oligomer formation (Fig. 4) support the results shown above: the speed of oligomer formation is significantly reduced with ePC as Hla binding lipid compared to eSM. Here, even at 40% ePC and eSM, respectively, a significant difference was observed. This can be ascribed to the lower toxin concentration employed (0.3 μM in Fig. 4 compared to 4 μM during incubation in Fig. 3a) and also one can expect that the differences are more pronounced at short reaction times. For 10% ePC only a very low level of oligomers forms in the first 300 s. For eSM the kinetics of excimer formation could be measured for 5%, 7%, 10% and 40% eSM. The apparent initial rate constants increase with increasing fraction of eSM (from $k_{obs} = 0.0025\ s^{-1}$ to 0.007 s^{-1} over 0.0251 s^{-1} and 0.030 s^{-1}). Thus as expected based on Eq. (A6) a positive correlation between α and k_{obs} is observed.

3.3. Role of Hla-binding lipid type and lipid phase

In the experiments described above, two different lipids (PC and SM) were compared which are in two different regimes with respect to their phase transition temperature T_{trans} relative to the experimental temperature T_{exp} (SM: $T_{exp} < T_{trans}$, PC: $T_{exp} > T_{trans}$). Thus, in order to

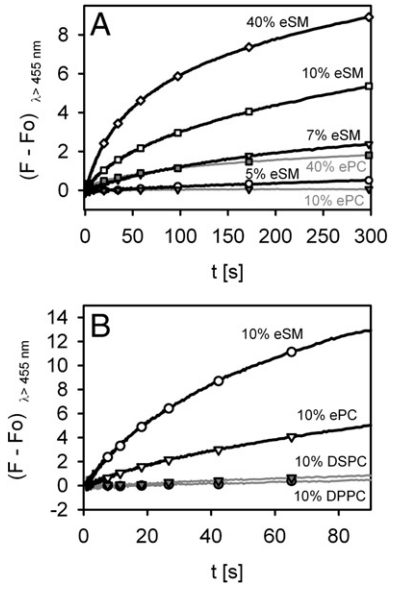

Fig. 4. Dependence of oligomerisation kinetics on surface density of binding sites. Liposomes containing 40% cholesterol and variable fractions of Hla binding lipids (17 μM in the outer leaflet) were rapidly mixed with fluorescently labelled toxin (0.3 μM) at 20 °C. The relative amount of Hla-binding lipids is indicated, non-binding lipids (ePE and bPS, 1:1) are used to fill up to 100%. Panel A: eSM (black lines) and ePC (grey lines), relative amounts as indicated. Panel B: 10% eSM and 10% ePC (black lines), 10% DPPC and DSPC (grey lines).

distinguish between the role of lipid phase and lipid type we additionally compared the interaction of Hla with PC-species where $T_{exp} < T_{trans}$ (DPPC, DSPC) and a SM species, where $T_{exp} > T_{trans}$ (OSM) at different relative amounts of Hla receptor lipid. Upon replacing ePC by DSPC or DPPC practically no oligomer formation was observed within the first 100 s (Fig. 4b) and also at later time points (2 h, 9 h) the level was well below the one observed for ePC (data not shown). In contrast, if conversely eSM is replaced by OSM the extent of oligomer formation remains on the same level in the pseudo-ternary/pseudo-binary mixtures but is higher for OSM in case of binary mixtures (Fig. 5a). The latter finding suggests that a liquid ordered phase as present in the binary mixture of eSM and cholesterol is less favourable for oligomerisation than a liquid disordered phase as present in case of OSM. The pattern observed with respect to the total extent of oligomer formation as represented by excimer fluorescence is reproduced if the amount of SDS stable oligomers is addressed by SDS–PAGE. The results for the whole set corresponding to Fig. 5a are shown in Fig. 5c, together with the gel from one subset of data (Fig. 5b). Except in the binary mixtures, the fraction of SDS stable oligomers for liposomes containing eSM or OSM is very similar. Unlike pyrene-excimer formation, the temperature dependence of the formation of SDS stable oligomers is very pronounced, as was also seen in Fig. 3a. Interestingly, a binary mixture of OSM with cholesterol is less efficient in inducing excimer formation than pseudo-binary mixtures containing additionally ePE and bPS, especially with respect to formation of SDS-stable oligomers.

3.4. Phase separation behaviour of pseudo-ternary mixtures

In case of phase separation the local density of binding sites will deviate from their average density. To check the mixtures employed in our binding studies for domain formation GUVs composed of cholesterol, ePS, ePE and ePC, eSM, DPPC or OSM were produced with 0.1% Lissamin-Rhodamin-DOPE as fluorescent lipid (Fig. 6). This lipid usually partitions preferentially into the liquid-disordered phase [20]. Despite the rather high cholesterol content phase separation was observed in these mixtures if high TM-lipids were used (DPPC, eSM) whereas for low-Tm-lipids (ePC, OSM) no phase separation seems to occur. In case of ePC it was shown that also in LUVs no phase separation occurs [21].

3.5. Temperature dependence of oligomer formation

The weak dependence of oligomer formation on temperature as revealed in Fig. 3a was supported by kinetic experiments (Fig. 7). The initial reaction rates show an increase with temperature (0.028 s^{-1},

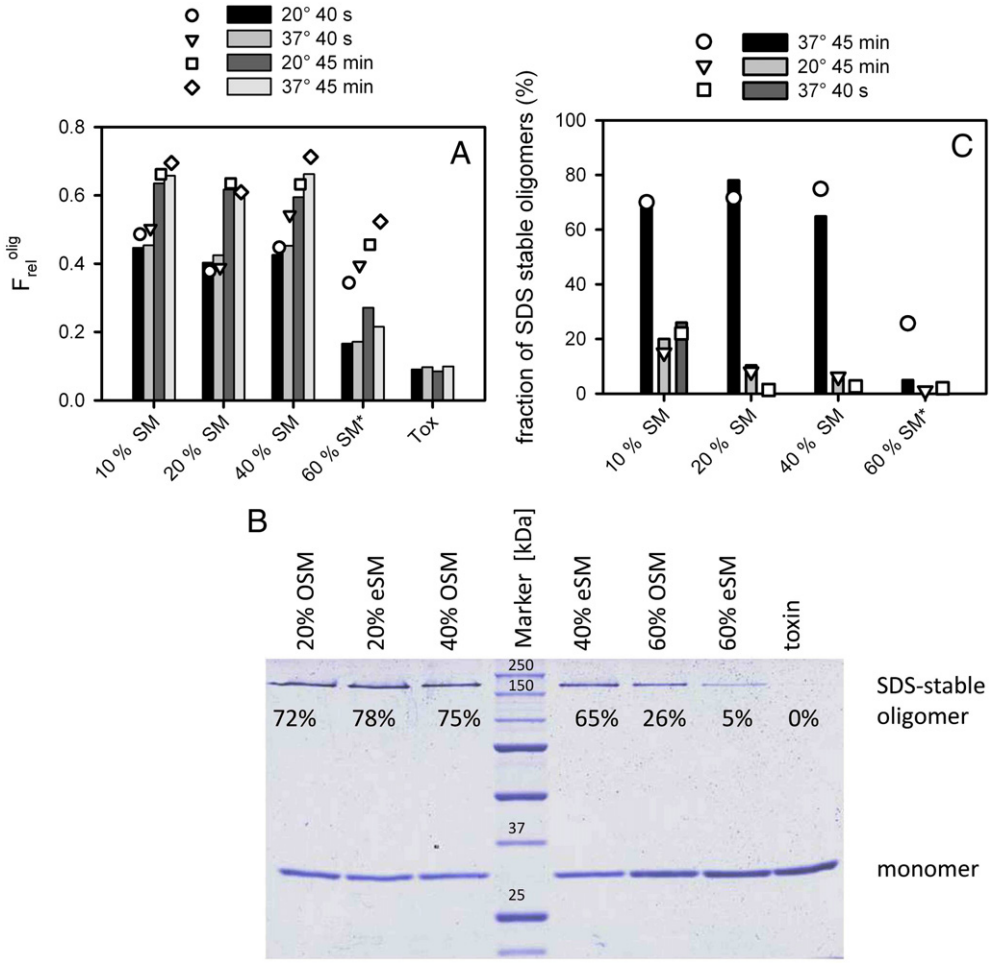

Fig. 5. Role of fluidity for Hla–SM interaction. Liposomes containing 40% cholesterol and variable fractions of two types of sphingomyelin (17 μM in the outer leaflet) were incubated for 40 s or 45 min at 20 °C or 37 °C with 4 μM pyrene labelled Hla. The rest of the lipid consists of ePE and bPS in a ratio of 1: 1. Panel A: Relative excimer fluorescence as obtained for pseudo-ternary and pseudo-binary mixtures (10, 20 and 40% SM with 40% cholesterol and 1: 1 ePE/bPS) and binary mixtures (60% SM with 40% cholesterol, indicated by a star). Samples were diluted to 0.1 μM directly before measurement. Bars indicated liposomes containing eSM, symbols (squares, triangles, circles, diamond) represent liposomes containing OSM as Hla-binding lipid. For comparison, fluorescence levels measured in absence of liposomes ("toxin") are depicted. After incubation, aliquots of the samples were subjected to 10% SDS–PAGE without heating. A gel showing part of the samples (45 min, 37 °C) is depicted in panel B; the numbers represent the fraction of oligomers based on a densitometric analysis (Quantity One, Bio-Rad, München, Germany). The results for all samples are depicted in panel C, with bars indicating liposomes containing eSM and symbols indicating liposomes containing OSM. Incubation time and temperature was as given in the legend. Marker: Precision Plus Protein unstained Standards (Bio-Rad, München, Germany).

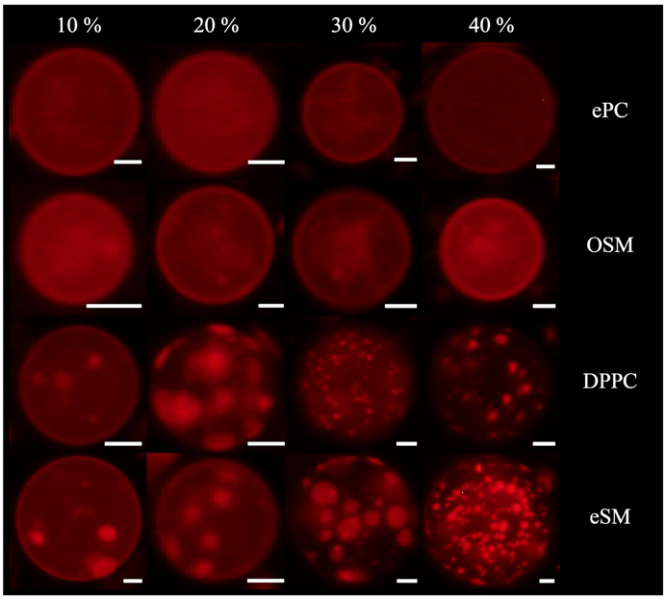

Fig. 6. Fluorescence microscopy of GUVs with pseudo-binary and pseudo-ternary mixtures. GUVs containing 40% cholesterol, fraction of Hla binding lipid as indicated and 1:1 ePE/bPS were analysed with respect to phase separation properties. GUVs with ePC and OSM show no phase separation, whereas GUVs with DPPC and eSM show phase separation. The bright regions indicate areas in the fluid disordered phase due to preferential partitioning of Lissamine rhodamine-DOPE (0.1 mol %) therein. Scale bars indicate 5 μM.

0.037 s^{-1} and 0.108 s^{-1}) but the overall oligomerisation level is similar for 4 °C, 22 °C and 37 °C. In contrast, efflux of encapsulated dye is strongly temperature dependent with barely any efflux at 4 °C and a significant difference between 22 °C and 37 °C (Fig. 7). Since pores are SDS stable, this corresponds to the pronounced difference between 20 °C and 37 °C in the level of SDS-stable oligomers (Fig. 3a).

4. Discussion

It is well established that binding of Hla from *S. aureus* to lipid membranes occurs only in presence of lipids with a phosphocholine headgroup, namely SM or PC, at least at neutral and basic pH [6,22]. Most studies have been performed either with vesicles composed of one type of lipid or with binary mixtures of cholesterol and lipid.

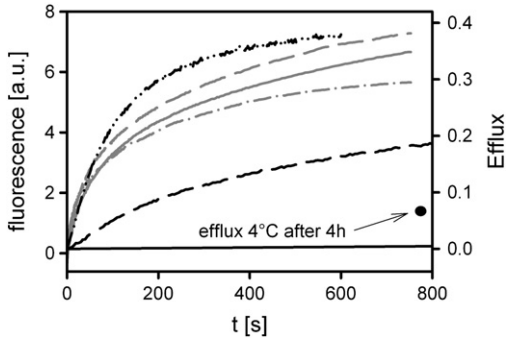

Fig. 7. Temperature dependence of kinetics of Hla–liposome interaction. Liposomes containing 40% cholesterol, 40% eSM, 10% ePE and 10% bPS (17 μM eSM in the outer leaflet) were rapidly mixed with fluorescently labelled toxin (0.3 μM) at 4 °C, 20 °C and 37 °C to follow oligomer formation (grey lines). The kinetics of pore formation was followed based on efflux of a self-quenching dye at the same temperatures. One hundred percent efflux was determined by addition of 10% Triton-X100. Solid line: 4 °C; dashed line: 22 °C; dotted-dashed line: 37 °C. Fluorescence is corrected for pure temperature effects.

Preferential binding of Hla to SM or PC was not reported for these liposomes. More recent experiments employing pseudo-ternary mixtures seemed to indicate that clustering of phosphocholine carrying lipids reduces effectively the concentration of toxin necessary to obtain measurable amounts of bound toxin [14]. In case of Hla the oligomerisation efficiency was considered to be a crucial parameter for determining the susceptibility of cells since based on competition experiments [6,14] it was concluded that the interaction between phosphocholine and Hla monomer is weak and clear indications for a high-affinity interaction with proteins on the cellular membrane are not reported. By investigating the oligomerisation behaviour of Hla under controlled conditions and model based interpretation of the results we were able to characterise the Hla–lipid interaction in more detail.

In support of the inhibition studies, our study clearly shows that the initial contact of monomeric Hla with lipids in artificial membranes occurs with low affinity, with dissociation constants in the higher μM range. In consequence measurable binding occurs only if oligomerisation takes place, thus the distinction between monomer affinity and oligomer affinity is difficult. Another consequence of the low affinity is that the amount of bound toxin increases with increasing concentration of Hla-binding lipids (see Appendix A). Thus, for a meaningful comparison of the effects of surface density it is crucial to adjust liposome concentration to yield the same molar concentration of Hla-binding sites. In our study this was taken into account for the first time. Thus, our results unambiguously show that increased oligomerisation can be induced by increasing the surface density of Hla binding lipids. According to Eqs. (A4) and (A6) increasing the surface density of binding sites (α) has the same effect as an increase in the dimerisation constant (K_{dim}), since both parameters occur always as product. Thus the increase in oligomerisation as shown in Fig. 3A can be attributed to the increase in surface density assuming that the oligomerisation constant is the same for the same type of lipid at different compositions. This might not be exactly the case: some effect of membrane composition on the oligomerisation constant can be deduced from the somewhat reduced oligomerisation level found with binary mixtures compared to pseudo-binary mixtures in case of OSM (Fig. 5a).

Obviously, oligomerisation efficiency is higher in case of eSM containing liposomes than in those where ePC is the Hla-binding lipid. One possible reason is that in case of eSM phase separation occurs and thus locally the surface density of Hla binding lipids is increased. Indeed in mixtures containing ePC no phase separation was observed, while the mixture containing eSM formed domains. Thus, the increased oligomerisation level in case of eSM could be the consequence of phase separation. However, since replacement of eSM by OSM, which did not lead to phase separation, did not change significantly the oligomerisation level compared to eSM, we have to conclude that SM *per se* leads to higher levels of oligomers compared to PC. The observation that pseudo-binary mixtures containing OSM leads to similar oligomer levels as pseudo-ternary containing eSM indicates two counteracting tendencies: phase separation increases local surface density, thus increasing oligomerisation level, but formation of a liquid ordered phase reduces oligomer formation. The reducing effect of formation of a liquid ordered phase is very evident in the comparison of binary mixtures of eSM and OSM, respectively, with cholesterol. In case of PC as Hla-binding lipid this effect is even more pronounced: replacing ePC by DPPC increases the local surface density of binding sites as evidence by fluorescence microscopy but the oligomerisation level of Hla decreases: obviously the membrane properties in DPPC-enriched domains do not support oligomerisation. This agrees with studies with binary mixtures of PC and cholesterol below and above the transition temperature, where in case of liquid ordered phase the level of bound toxin was very low [23]. Overall these data clearly show that under similar conditions (ePC *versus* OSM, DPPC *versus* eSM) oligomerisation on membranes containing

SM occurs with significantly increased efficiency. Phase separation as process which increases local surface density might increase the efficiency to some extent, but is partially compensated by unfavourable conditions introduced by the transition to a liquid ordered phase.

The picture emerging from this study is that Hla similar to a number of other POC-dependent toxins [3–5] has some specificity for SM which was not detected up to now. Due to the rather low intrinsic affinity with respect to the initial monomer binding the apparent binding is strongly influenced by the efficiency of oligomer formation. Thus, the apparent binding constant (c_{50}) depends both on monomer binding affinity and oligomerisation constant. So far our model based data analysis indicates that preferential interaction of Hla to SM compared to PC results from a higher probability of oligomerisation rather than a higher affinity for monomer binding. Since a significant population of membrane bound toxin is only observed if oligomers are formed and bound monomers exist only in minor amounts, direct determination of the affinity for monomer binding is difficult.

Initial interaction of Hla with lipid membranes seems to occur via the POC-binding site as identified in the crystal structure of the heptameric pore and in the structure of the monomeric form of the closely related toxin LukF [8,9,24]. Since only the headgroup is recognised by this site it is unlikely that this interaction is the reason for specific binding to SM or PC, and this agrees with our result that monomer binding affinity for the two lipids might be similar in case of Hla. Thus, additional interactions between bound monomer and membrane must occur, possibly leading to different orientations of the bound monomer for the two types of lipids, which could explain different probabilities of oligomerisation.

In this study we could not distinguish between different oligomeric states on the membrane. However, the observation that no lag-phase in the kinetic traces was observed indicates that at least in this initial phase dimers, trimers etc. exist. Under equilibrium conditions possibly mainly heptameric oligomers exist: recent experiments indicated that the main membrane bound species after 30 min incubation are heptamers and that smaller oligomers are only weakly populated [25].

With respect to the initial lipid binding partner on the cell membrane or lipid "receptor" one has to conclude that due to the high relative content of unsaturated PC and saturated SM in the plasma membrane the surface density of binding sites is not likely to play a role for selective binding. Both in rabbit and human erythrocytes PC and SM together contribute more than 85% of the outer leaflet-lipids [26,27], with cholesterol contributing 0.8 mol/mol lipid in rabbits [26] and in humans [28]. Thus the surface density of the two lipids is not likely to differ very much and is well represented by the compositions containing 40% eSM and 40% ePC. Nevertheless, a preferential binding of Hla to SM in the cellular context can be expected due to an intrinsically higher overall affinity as evidenced by our liposome studies. Thus, removal of SM is expected to reduce cytotoxicity of Hla as has been observed [14]. However, a particular role for rafts cannot be deduced from this observation.

Acknowledgments

This work was supported by the DFG (SFB 490). We thank Prof. S. Bhakdi, Dr. A. Valeva and Prof. M. Husmann, Institute of Medical Microbiology and Hygiene, Medical University Center, Mainz, for help with production of the toxin, and Prof. H. Decker for constant support.

Appendix A. Dimerisation model

In order to be able to interpret the results on oligomer formation as monitored by excimer-fluorescence in more detail, we developed a model describing equilibrium concentration and kinetics of dimer formation. Ideally one would use a model describing all steps up to the final heptamer, but the large number of parameters defining such a model prevents this, since the values for these parameters are not known yet. However, since the aim of using this model is solely to understand the quantitative behaviour of such an oligomerisation process upon variation of Hla concentration, lipid-concentration etc., we used the minimal oligomer model (dimer model) which has the additional advantage, that the solution for kinetics and equilibrium are analytic and compact enough to allow an intuitive understanding. Otherwise an intensive screening of possible parameter combinations would be necessary, which is beyond the scope of this article. The set-up of the model is the same as used by [29].

Thus, we consider the following reaction scheme:

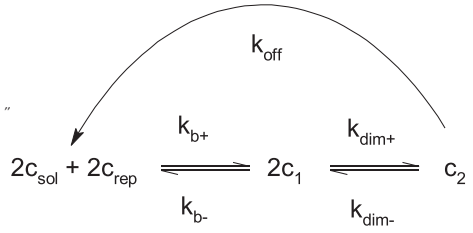

Binding of soluble monomers (c_{sol}) to lipid membranes occurs to specific toxin-binding lipids, denoted receptor lipids (c_{rep}). Bound monomers (c_1) can dimerize on the membrane. Dimers (c_2) can dissociate to bound monomers, or leave the membrane as dimer. In solution they rapidly dissociate into soluble monomers; thus the rate limiting step in this path is dissociation from the membrane (k_{off}). The dimerisation equilibrium constant is given by $K_{dim} = k_{dim+}/k_{dim-}$, the monomer binding constant by $K_b = k_{b+}/k_{b-}$.

Equilibrium model for dimerisation on the membrane

Surface densities (σ_x) of species x (x = 1 (monomer), 2 (dimer), tot (total toxin) or rep (receptor-lipid)) are expressed as number per nm^2 of membrane surface available where only the area of the outer leaflet is taken into account:

$$\sigma_x = \frac{c_x}{A_{ves} c_{ves}} = \frac{q}{A_{lip}} \frac{c_x}{c_{lip}} = r \frac{c_x}{c_{lip}}$$
$$C_{ves} = c_{lip}/N$$
$$N = qA_{ves}/A_{lip}$$

with A_{ves} = area of the outer leaflet of the vesicle, q = (area of inner + outer leaflet)/(area of the outer leaflet), $q \approx 1.8$ for $\varnothing_{liposome}$ = 100 nm, N = number of lipids per liposome, c_{lip} = concentration of lipids (mol/l) and A_{lip} the area per lipid. With typical values for A_{lip} (0.6 nm^2) one obtains at value of $r \approx 3$ nm^{-2}.

The surface concentration of dimers on the membrane is determined by the corresponding dimerisation constant (K_{dim}, units: nm^2) and the surface densities of monomers:

$$\sigma_2 = K_{dim} \sigma_1^2 \tag{A1}$$

The concentration of bound monomer is expressed by the respective equilibrium constant K_b, the concentration of toxin in solution (c_{sol}) and the concentration of lipids to which the toxin can bind ("receptor") which is only a fraction α of the total lipid ($c_{rep} = \alpha\, c_{lip}$):

$$c_1 = K_b c_{rep} c_{sol}$$

This can also be expressed in terms of surface concentrations with the appropriate binding constant K_{app}:

$$\sigma_1 = K_{app}\sigma_{sol}$$
$$K_{app} = K_b c_{rep} \quad (A2)$$

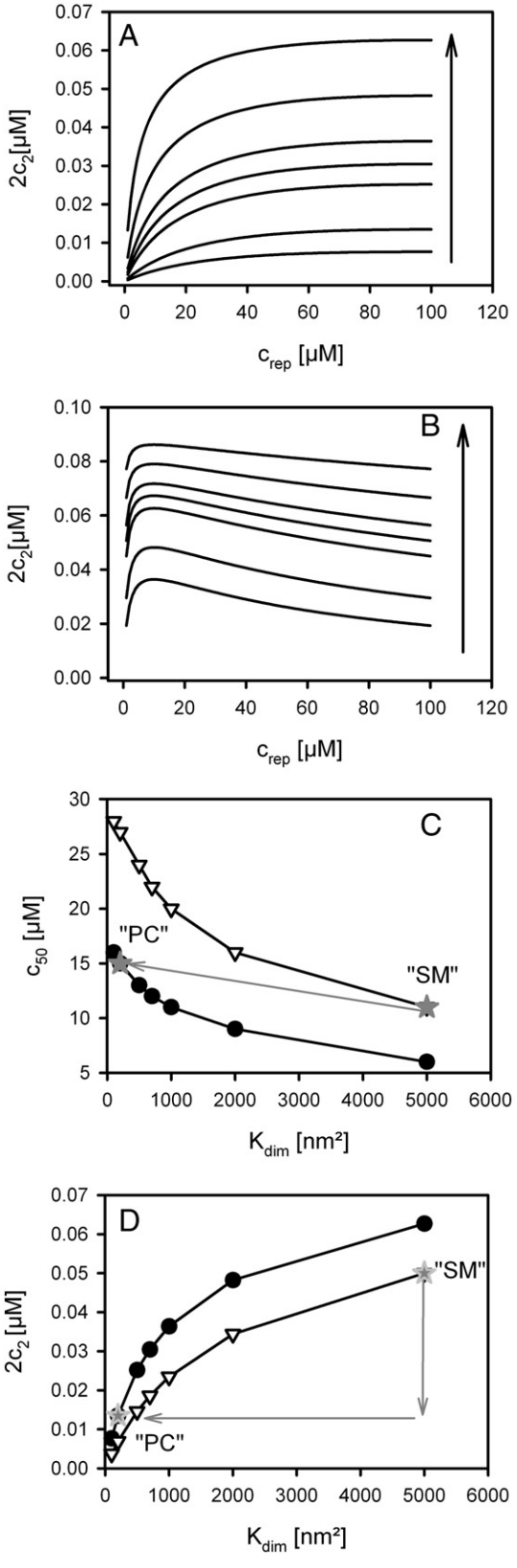

In the current situation (Fig. 2a) we may assume that $c_{rep} = c_{rep,total}$ due to the low concentration of toxin relative to receptor lipid. Mass balance is employed to solve for σ_1, yielding:

$$0 = \sigma_{sol} + \sigma_1 + 2\sigma_2 - \sigma_{tot} = 2K_{dim}\sigma_1^2 + \frac{\sigma_1}{\Theta} - \sigma_{tot} \qquad \Theta = \frac{K_{app}}{1+K_{app}}$$
$$\sigma_1 = \frac{1}{4\Theta K_{dim}}\left(\sqrt{1+8K_{dim}\Theta^2\sigma_{tot}} - 1\right) \quad (A3)$$

For a description of the type of data as shown in Fig. 2a we need the fluorescence signal F, which is proportional to the dimer concentration c_2, in dependence on receptor concentration c_{rep}. If the specific fluorescence signal is expressed per monomer and employing $c_2 = \sigma_2 c_{lip}/r$, we obtain:

$$F = F_o 2c_2 = F_o \frac{\left(1+K_b c_{rep}\right)^2}{K_{fit} c_{rep}}\left(\sqrt{1+K_{fit}\frac{c_{rep}}{\left(1+K_b c_{rep}\right)^2}c_o} - 1\right)^2 \quad (A4)$$
$$K_{fit} = 8K_{dim} r\alpha K_b^2$$

Eq. (A4) shows that the lipid dependence is mainly determined by the product $K_{dim}K_b^2$, especially if $c_{rep} < 1/K_b$. Thus it is difficult to separate the effect of changes in experimental conditions on the dimerisation constant from those on the monomer binding constant.

This function has a maximum at $c_{rep} = 1/K_b$. At values of $c_{rep} > 1/K_b$ the level decreases due to surface dilution. However, this decrease is only observed if K_b is not too low and K_{dim} not too high. This is depicted in Fig. A1a and b, were for two values of K_b the binding curves for different dimerisation constants are compared. In case of $K_b = 0.01\ \mu M^{-1}$ typical saturation curves result up to 100 µM lipid (Fig. A1a), whereas for $K_b = 0.1\ \mu M^{-1}$ a decrease of dimer level at increased lipid concentration is observed (Fig. A1b). Also for $K_b = 0.01\ \mu M^{-1}$ a decrease in saturation level occurs at lipid concentrations >100 µM; only at very high dimerisation constants this effect is nearly absent. This effect can be seen also in Fig. A1b: the higher the dimerisation constant the less pronounced the decrease in dimer level at increased lipid concentration.

The function describing the maximal concentration of dimers at $c_{rep} = 1/K_b$ is given by:

$$c_{2,max} = \frac{1}{2}\left(c_{tot} + \frac{1-\sqrt{1+2bc_{tot}}}{b}\right)$$
$$b = r\alpha K_{dim} K_b$$

Thus, the maximal value is constant, if the product of monomer binding affinity K_b, dimerisation constant K_{dim} and fraction of receptor lipids α, which reflects the surface density of binding sites, is constant.

The effect of changing K_b and K_{dim} on the expected dimer level at 100 µM lipid ($2c_2$) and the concentration to achieve half of this level (c_{50}) is depicted in Fig. A1c and d. The compensating effect of increasing K_b and simultaneously decreasing K_{dim} can be verified in Fig.A1d: the values for c_2 at 100 µM lipid, which is close to the maximal level at these conditions, is the very similar for $K_b = 0.005\ \mu M^{-1}$ and $K_{dim} = 5000\ nm^2$ and $K_b = 0.01\ \mu M^{-1}$ and $K_{dim} = 2500\ nm^2$, respectively.

Fig. A1. Simulation of dimerisation behaviour on a membrane. Dimer concentration in dependence on receptor concentration was simulated based on the model described in the Appendix for $c_{tot} = 0.1$ µM, $\alpha = 0.6$, $r = 3$, and variable values for K_b and K_{dim}. Panel A: monomer binding constant $K_b = 0.01\ \mu M^{-1}$ and $K_{dim} = 100, 200, 500, 700, 1000, 2000, 5000\ nm^2$, increasing in direction of the arrow; panel B: $K_b = 0.1\ \mu M^{-1}$; K_{dim} as in panel A; panel C: c_{50} values for the curves in panel A ($K_b = 0.01\ \mu M^{-1}$, closed circles) and for $K_b = 0.005\ \mu M^{-1}$, open triangles. The stars indicate the c_{50} values found in the experiments for eSM and ePC, respectively. Panel D: levels of dimer formation (c_2) at 100 µM receptor lipid for the same simulation as basis for panel D. Stars indicate positions with similar relative amount of dimers as found for the relative intensity of excimer fluorescence in the experiments with liposomes containing ePC and eSM, respectively (Fig. 2a).

Furthermore, we can support based on these figures, that most likely the main difference in Hla-interaction with eSM and ePC is increased oligomerisation efficiency in case of eSM. A slight increase of c_{50} from 11 to 15 μM (Fig. A1c, stars) and a strong reduction of dimer level ($2c_2$, Fig. A1d, stars) is compatible with an increase in monomer binding affinity by a factor of 2 (from $K_b = 0.005$ to 0.01 μM^{-1}) and a decrease in dimerisation constant by a factor of 25 (from 5000 to 200 nm^2). If monomer binding affinity was the same for both lipids, the c_{50} should have changed much more in order to be compatible with a strong decrease in dimer level.

Kinetics of dimerisation

For the dimerisation process we may write

$$\frac{d}{dt}\sigma_2 = k_{\dim+}\sigma_1^2 - (k_{\dim-} + k_{off})\sigma_2 := k_{\dim+}\sigma_1^2 - k_-\sigma_2 \quad (A5)$$

If monomer binding is much faster than dimerisation, the monomers on the membrane are in a rapid equilibrium with soluble monomers and can be expressed as:

$$\sigma_1 = (\sigma_{tot} - 2\sigma_2)\Theta$$

Substitution of σ_1 into Eq. (A5) yields:

$$\frac{d}{dt}\sigma_2 = k_{\dim+}\Theta^2\sigma_{tot}^2 - k_{\dim+}\Theta^2\sigma_2 4(\sigma_{tot} - \sigma_2) - k_-\sigma_2$$

Since in the initial phase we can approximate $\sigma_{tot} - \sigma_2 \approx \sigma_{tot}$

$$\frac{d}{dt}\sigma_{2,ini} = k_{\dim+}\Theta^2\sigma_{tot}^2 - \left(k_{\dim+}\Theta^2 4\sigma_{tot} + k_-\right)\sigma_2$$

Substituting for molar concentrations yields

$$\frac{d}{dt}c_{2,ini} = k_{\dim+}\left(\frac{K_b}{K_b c_{rep}+1}\right)^2 c_{rep} r\alpha c_{tot}^2 - \left(k_{\dim+}\left(\frac{K_b}{K_b c_{rep}+1}\right)^2 c_{rep} 4r\alpha c_{tot} + k_-\right)c_2$$

The solution for this differential equation is a simple exponential function with a time constant of

$$k_{obs} = 4rk_{\dim+}\alpha\left(\frac{K_b}{K_b c_{rep}+1}\right)^2 c_{rep}c_{tot} + k_- := k_{+,app} + k_- \quad (A6)$$

Thus, the observed time constant in the initial phase of the reaction should increase with c_{tot} and α, as was observed in the experiments.

The dependence on c_{rep} is non-monotonous: for $K_b c_{rep} << 1$, a linear increase is expected; for $K_b c_{rep} >> 1$ a decrease of $k_{+,app}$ according to $1/c_{rep}$ is expected. Thus, at a certain concentration c_{rep} the effective dissociation rate ($k_- = k_{\dim-} + k_{off}$) will dominate ($k_- >> k_{+,app}$) and k_{obs} will not depend measurably on c_{rep}. The maximal value for $k_{+,app}$ will be obtained at $1/K_b = c_{rep}$.

We observe a positive correlation of k_{obs} with c_{rep}, indicating that $K_b c_{rep} << 1$. The lowest value of k_{obs} is about 0.01 s^{-1}, thus $k_- < 0.01\ s^{-1}$ corresponding to a half life of 100 s. Since $k_- = k_{\dim-} + k_{off}$ we can estimate that the half life of the dimer is longer than 100 s.

Fit equations for data in Fig. 2

Hyperbolic function

$$F = F_o\frac{c_{rep}}{c_{rep} + c_{50}} \quad (A7)$$

Hill-Equation

$$F = F_o\frac{c^n{}_{rep}}{c^n{}_{rep} + c^n{}_{50}} \quad (A8)$$

Maximal number of toxin monomers per liposome

If we approximate the pore structure by a cylinder with a diameter of 10 nm the area is about 80 nm^2. Considering an area of 0.6 nm^2 per lipid (average between POPC and SM, [26]), this corresponds to 130 lipid molecules, or 16 per monomer (a monomer in the pore structure roughly occupies 1/8 of the pore structure due to the channel). Thus, if for example liposomes with 40% eSM and 40% cholesterol are considered, with an eSM concentration of 2.5 μM in the outer leaflet, the total lipid concentration is 3.8 μM, which could accommodate 3.8/16 = 0.24 μM toxin. Here, we assume that cholesterol does not contribute to the lipid area, since it rather has a condensing effect [30]. At an eSM concentration of 17 μM (compare Fig. 3) the limiting concentration of bound toxin would be 1.6 μM.

References

[1] I. Iacovache, F.G. van der Goot, L. Pernot, Pore formation: an ancient yet complex form of attack, Biochim. Biophys. Acta 1778 (2008) 1611–1623.
[2] M.R. Gonzalez, M. Bischofberger, L. Pernot, F.G. van der Goot, B. Freche, Bacterial pore-forming toxins: the (w)hole story? Cell Mol. Life Sci. 65 (2008) 493–507.
[3] H. Shogomori, T. Kobayashi, Lysenin: a sphingomyelin specific pore-forming toxin, Biochim. Biophys. Acta 1780 (2008) 612–618.
[4] K.C. Kristan, G. Viero, M. Dalla Serra, P. Macek, G. Anderluh, Molecular mechanism of pore formation by actinoporins, Toxicon 54 (2009) 1125–1134.
[5] B. Bakrac, I. Gutierrez-Aguirre, Z. Podlesek, A.F. Sonnen, R.J. Gilbert, P. Macek, J.H. Lakey, G. Anderluh, Molecular determinants of sphingomyelin specificity of a eukaryotic pore-forming toxin, J. Biol. Chem. 283 (2008) 18665–18677.
[6] M. Watanabe, T. Tomita, T. Yasuda, Membrane-damaging action of staphylococcal alpha-toxin on phospholipid-cholesterol liposomes, Biochim. Biophys. Acta 898 (1987) 257–265.
[7] S. Galdiero, M. Galdiero, C. Pedone, beta-Barrel membrane bacterial proteins: structure, function, assembly and interaction with lipids, Curr. Protein Pept. Sci. 8 (2007) 63–82.
[8] L. Song, M.R. Hobaugh, C. Shustak, S. Cheley, H. Bayley, J.E. Gouaux, Structure of staphylococcal alpha-hemolysin, a heptameric transmembrane pore, Science 274 (1996) 1859–1866.
[9] S. Galdiero, E. Gouaux, High resolution crystallographic studies of alpha-hemolysin-phospholipid complexes define heptamer-lipid head group interactions: implication for understanding protein-lipid interactions, Protein Sci. 13 (2004) 1503–1511.
[10] A. Hildebrand, M. Pohl, S. Bhakdi, *Staphylococcus aureus* alpha-toxin. Dual mechanism of binding to target cells, J. Biol. Chem. 266 (1991) 17195–17200.
[11] I. Maharaj, H.B. Fackrell, Rabbit erythrocyte band 3: a receptor for staphylococcal alpha toxin, Can. J. Microbiol. 26 (1980) 524–531.
[12] S. Pany, R. Vijayvargia, M.V. Krishnasastry, Caveolin-1 binding motif of alpha-hemolysin: its role in stability and pore formation, Biochem. Biophys. Res. Commun. 322 (2004) 29–36.
[13] G.A. Wilke, J.B. Wardenburg, Role of a disintegrin and metalloprotease 10 in *Staphylococcus aureus* alpha-hemolysin-mediated cellular injury, Proc. Natl. Acad. Sci. U. S. A. 107 (2010) 13473–13478.
[14] A. Valeva, N. Hellmann, I. Walev, D. Strand, M. Plate, F. Boukhallouk, A. Brack, K. Hanada, H. Decker, S. Bhakdi, Evidence that clustered phosphocholine head groups serve as sites for binding and assembly of an oligomeric protein pore, J. Biol. Chem. 281 (2006) 26014–26021.
[15] A. Valeva, J. Pongs, S. Bhakdi, M. Palmer, Staphylococcal alpha-toxin: the role of the N-terminus in formation of the heptameric pore — a fluorescence study, Biochim. Biophys. Acta 1325 (1997) 281–286.
[16] M. Schwiering, N. Hellmann, Validation of liposomal lipid composition by thin layer chromatography, J. Liposome Res. 22 (2012) 279–284.
[17] A.G. Therien, C.M. Deber, Interhelical packing in detergent micelles. Folding of a cystic fibrosis transmembrane conductance regulator construct, J. Biol. Chem. 277 (2002) 6067–6072.
[18] U.K. Laemmli, Cleavage of structural proteins during the assembly of the head of bacteriophage T4, Nature 227 (1970) 680–685.
[19] D.H. Kang, Y.S. Gho, M.K. Suh, C.H. Kang, Highly sensitive and fast protein detection with coomassie brilliant blue in sodium dodecyl sulfate-polyacrylamide gel electrophoresis, Bull. Kor. Chem. Soc. 23 (2002) 1511–1512.
[20] T. Baumgart, G. Hunt, E.R. Farkas, W.W. Webb, G.W. Feigenson, Fluorescence probe partitioning between Lo/Ld phases in lipid membranes, Biochim. Biophys. Acta 1768 (2007) 2182–2194.
[21] T.Y. Wang, J.R. Silvius, Cholesterol does not induce segregation of liquid-ordered domains in bilayers modeling the inner leaflet of the plasma membrane, Biophys. J. 81 (2001) 2762–2773.
[22] B. Vecsey-Semjen, R. Mollby, F.G. van der Goot, Partial C-terminal unfolding is required for channel formation by staphylococcal alpha-toxin, J. Biol. Chem. 271 (1996) 8655–8660.

[23] T. Tomita, M. Watanabe, T. Yasuda, Influence of membrane fluidity on the assembly of *Staphylococcus aureus* alpha-toxin, a channel-forming protein, in liposome membrane, J. Biol. Chem. 267 (1992) 13391–13397.
[24] R. Olson, H. Nariya, K. Yokota, Y. Kamio, E. Gouaux, Crystal structure of staphylococcal LukF delineates conformational changes accompanying formation of a transmembrane channel, Nat. Struct. Biol. 6 (1999) 134–140.
[25] J.R. Thompson, B. Cronin, H. Bayley, M.I. Wallace, Rapid assembly of a multimeric membrane protein pore, Biophys. J. 101 (2011) 2679–2683.
[26] G.J. Nelson, Lipid composition of erythrocytes in various mammalian species, Biochim. Biophys. Acta 144 (1967) 221–232.
[27] J.A. Virtanen, K.H. Cheng, P. Somerharju, Phospholipid composition of the mammalian red cell membrane can be rationalized by a superlattice model, Proc. Natl. Acad. Sci. U. S. A. 95 (1998) 4964–4969.
[28] D. Hegner, D. Platt, H. Heckers, U. Schloeder, V. Breuninger, Age-dependent physiochemical and biochemical studies of human red cell membranes, Mech. Ageing Dev. 10 (1979) 117–130.
[29] V.T. Nguyen, Y. Kamio, H. Higuchi, Single-molecule imaging of cooperative assembly of gamma-hemolysin on erythrocyte membranes, EMBO J. 22 (2003) 4968–4979.
[30] G. Lindblom, G. Oradd, Lipid lateral diffusion and membrane heterogeneity, Biochim. Biophys. Acta 1788 (2009) 234–244.